Heliyon 10 (2024) e34530

Contents lists available at ScienceDirect

Heliyon

journal homepage: www.cell.com/heliyon

Research article

Identification and experimental verification of immune-related hub genes in intervertebral disc degeneration

Zeling Huang [a,1], Xuefeng Cai [a,1], Xiaofeng Shen [a,b,1], Zixuan Chen [a], Qingtian Zhang [a], Yujiang Liu [a], Binjie Lu [a], Bo Xu [a,**], Yuwei Li [a,b,*]

[a] Suzhou TCM Hospital Affiliated to Nanjing University of Chinese Medicine, Suzhou, Jiangsu, 215009, China
[b] Orthopaedic Traumatology Institute, Suzhou Academy of Wumen Chinese Medicine, Suzhou, Jiangsu, 215009, China

ARTICLE INFO

Keywords:
Intervertebral disc degeneration
Bioinformatics analysis
Machine learning
Immune
Nucleus pulposus

ABSTRACT

Background: Inflammation and immune factors are the core of intervertebral disc degeneration (IDD), but the immune environment and epigenetic regulation process of IDD remain unclear. This study aims to identify immune-related diagnostic candidate genes for IDD, and search for potential pathogenesis and therapeutic targets for IDD.

Methods: Gene expression datasets were obtained from the Gene Expression Omnibus (GEO). Differential expression immune genes (Imm-DEGs) were identified through weighted gene correlation network analysis (WGCNA) and linear models for microarray data analysis (Limma). LASSO algorithm was used to identify feature genes related to IDD, which were compared with core node genes in PPI network to obtain hub genes. Based on the coefficients of hub genes, a risk model was constructed, and the diagnostic value of hub genes was further evaluated through receiver operating characteristic (ROC) analysis. Xcell, an immunocyte analysis tool, was used to estimate the infiltration of immune cells. Finally, nucleus pulposus cells were co-cultured with macrophages to create an M1 macrophage immune inflammatory environment, and the changes of hub genes were verified.

Results: Combined with the results of WGCNA and Limma gene differential analysis, a total of 30 Imm-DEGs were identified. Imm-DEGs enriched in multiple pathways related to immunity and inflammation. LASSO algorithm identified 10 feature genes from Imm-DEGs that significantly affected IDD, and after comparison with core node genes in the PPI network of Imm-DEGs, 6 hub genes (NR1H3, SORT1, PTGDS, AGT, IRF1, TGFB2) were determined. Results of ROC curves and external dataset validation showed that the risk model constructed with the 6 hub genes had high diagnostic value for IDD. Immunocyte infiltration analysis showed the presence of various dysregulated immune cells in the degenerative nucleus pulposus tissue. In vitro experimental results showed that the gene expression of NR1H3, SORT1, PTGDS, IRF1, and TGFB2 in nucleus pulposus cells in the immune inflammatory environment was up-regulated, but the change of AGT was not significant.

* Corresponding author. Suzhou TCM Hospital Affiliated to Nanjing University of Chinese Medicine, Suzhou, Jiangsu, 215009, China.
** Corresponding author. Suzhou Hospital of Traditional Chinese Medicine, 18 Yangsu Road, Canglang New City, Suzhou City, Jiangsu Province, China.
E-mail addresses: xubo12080@163.com (B. Xu), lyw97538@126.com (Y. Li).
[1] These authors have contributed equally to this work and share first authorship.

https://doi.org/10.1016/j.heliyon.2024.e34530
Received 20 March 2024; Received in revised form 10 July 2024; Accepted 10 July 2024
Available online 11 July 2024

Conclusions: The hub genes NR1H3, SORT1, PTGDS, IRF1, and TGFB2 can be used as immunorelated biomarkers for IDD, and may be potential targets for immune regulation therapy for IDD.

1. Background

Low back pain is one of the most common orthopedic diseases in clinical practice, affecting approximately 40 % of the global population. It is an important medical condition that affects the quality of life of the elderly and causes a huge social and economic burden [1]. The intervertebral disc is the largest avascular tissue area in the human body and is mainly composed of the central nucleus pulposus, lateral annulus fibrosus, and upper and lower cartilage endplates. Intervertebral disc degeneration (IDD) is the most common cause of low back pain and can lead to various spinal diseases, such as structural instability, disc herniation, spinal stenosis, nerve root disease, and myelopathy [2]. IDD is related to genetics, lifestyle, and aging. The main pathological features of IDD include the release of proinflammatory factors, gradual loss of extracellular matrix, increased cellular death, and changes in the phenotype of healthy intervertebral disc cells [3,4]. However, the etiology and pathogenesis of this disease are still not completely understood.

Currently, there are three main theories that explain the pathophysiology of IDD: mechanical compression theory, chemical nerve root inflammation theory, and autoimmune theory. Immune privileged organs are those that do not come into contact with immune cells during development. In these organs, there are isolation barriers between the internal environment and the body's immune system, such as the blood-brain barrier and blood-eye barrier. Since its formation, the nucleus pulposus has been enclosed within the annulus fibrosus and cartilaginous endplate, creating a unique structure that isolates it from the body's immune system. Exposing the various components of the nucleus pulposus to the body's immune system can trigger an autoimmune reaction. Therefore, the intervertebral disc is considered an immune-privileged organ [5–7]. In fact, the concept of intervertebral disc immune privilege has been proposed for many years. However, to date, our understanding of the mechanisms behind intervertebral disc immune privilege and its clinical significance remains unclear. In 2002, Burke et al. proposed that degenerated intervertebral disc tissue produces proinflammatory mediators and cytokines, giving rise to the chemical radiculitis theory [8]. From a microscopic perspective, both the chemical radiculitis theory and the autoimmunity theory to a large extent explain the pathophysiology of IDD by suggesting that inflammation and immune factors are at the core of pain and spinal degeneration. However, the role of the immune environment and epigenetic regulation in the pathological process of IDD is still not clear.

Transcriptomics and machine learning are becoming increasingly mature in their application to bioinformatics [9–11]. The analysis of molecular networks and genes can enhance our overall understanding of IDD [12]. In this study, we first downloaded IDD-related data sets from the Gene Expression Omnibus (GEO) database and obtained immune-related genes from the ImmPort and GeneCards databases. Differentially expressed genes (DEGs) were identified by weighted gene correlation network analysis (WGCNA) and linear models for microarray data analysis (Limma). Machine learning was used to determine the hub immune-related diagnostic biomarkers for IDD. Immune cell infiltration analysis was conducted to observe the immune cell infiltration characteristics of IDD. Changes in hub genes were verified through cell experiments. This study may help identify potential immunodiagnostic and therapeutic biomarkers for IDD.

2. Materials and methods

2.1. Microarray data source

Search the GEO database (https://www.ncbi.nlm.nih.gov/geo/) for studies involving 'intervertebral disc degeneration' and apply subsequent screening criteria, including experiment type (array expression profile), species (Homo sapiens), sample source (nucleus pulposus tissue or whole blood), and modeling time. Ultimately, the dataset of interest, GSE70362 [13], GSE147383 [14], GSE56081 [15] and GSE124272 [16], was selected for further analysis. The GSE70362 chip data includes 16 IDD samples and 8 control samples, the GSE147383 chip data includes 2 IDD samples and 2 control samples, and the GSE56081 chip data includes 5 IDD samples and 5 control samples. These three datasets are used for analysis. The GSE124272 chip data includes 8 IDD samples and 8 control samples, and this dataset is used for hub gene validation (Table 1). Import those datasets into the Sangerbox platform (http://sangerbox.com/home.html) for subsequent correlation analysis [17]. We normalized the gene expression data using the R package "optparse" [18]. The inSilicoMerging R package (DOI: 10.1186/1471-2105-13-335) was used to merge the three datasets, and then batch effects were removed using Johnson WE et al.'s method [19]. Specifically, we estimate the Location and scale model parameters that represent the

Table 1
Microarray data.

Data number	Platform information	IDD group	Control group	Species	Tissu
GSE70362	GPL17810	16	8	Homo sapien	Nnucleus pulposus
GSE147383	GPL570	2	2	Homo sapien	Nnucleus pulposus
GSE56081	GPL15314	5	5	Homo sapien	Nnucleus pulposus
GSE124272	GPL21185	8	8	Homo sapien	whole blood

batch effects by "pooling information" across genes in each batch to 'shrink' the batch effect parameter estimates toward the overall mean of the batch effect estimates (across genes). These empirical Bayes estimates are then used to adjust the data for batch effects, providing more robust adjustments for the batch effect on each gene.

We obtained 1793 and 17767 immune-related genes from the ImmPort [20] and GeneCards [21] databases, respectively. From the intersection of these two gene sets, 1698 immune-related genes were identified.

2.2. Weighted gene correlation network analysis

We used the 'WGCNA' package in R software to study the association between genes and phenotypes by constructing gene co-expression networks [22]. The Median Absolute Deviation (MAD) of each gene was calculated separately, excluding the top 50 % of genes with the smallest MAD. Then, both Pearson's correlation matrices and average linkage method were applied for all pairwise genes. Next, a weighted adjacency matrix was constructed using a power function A_mn = |C_mn|^β (C_mn = Pearson's correlation between Gene_m and Gene_n; A_mn = adjacency between Gene m and Gene n). To classify genes with similar expression profiles into gene modules, average linkage hierarchical clustering was conducted according to the TOM-based dissimilarity measure with a minimum size of 300 for the gene group dendrogram, and a sensitivity set to 3. In addition, we also incorporated modules with distances less than 0.25.

2.3. Identification of immunodifferentially expressed genes associated with IDD

Perform differential analysis using the R software package limma (https://doi.org/10.1093/nar/gkv007, version 3.40.6) to obtain differentially expressed genes [23]. Specifically, we obtained the expression profile dataset, used the lmFit function for multiple linear regression, further used eBayes function to compute moderated t-statistics, moderated F-statistic, and log-odds of differential expression by empirical Bayes moderation of the standard errors towards a common value, and ultimately obtained the significance of differential expression for each gene. The differential gene screening threshold was set as follows: fold change>1.5, *P*-value<0.05. Volcano plots and heatmaps were used to display the results of differential gene expression. The intersection of DEGs and immune genes was taken to obtain the differentially expressed immune genes (Imm-DEGs).

2.4. Enrichment analysis

The 'clusterProfile' package [24] in R software was used to explore the biological functions of Imm-DEGs. We performed gene ontology (GO) and kyoto encyclopedia of genes and genomes (KEGG) analysis [25,26]. Set the minimum gene set to 5 and the maximum to 5000,*P* value of <0.05 and a FDR of <0.25 were considered statistically significant.

2.5. Protein-protein interaction (PPI) network

The PPI relationship of Imm-DEGs was obtained by using String database. Cytoscape 3.7.2 software was used to construct the protein-protein interaction network diagram [27]. Network topology analysis was performed using the 'CytoNCA' app in the software, and core node genes were selected based on betweenness centrality. Genes in the top 50 % of the betweenness centrality of the PPI network are screened as the core node genes of the network.

2.6. Identification of candidate hub genes via machine learning

We integrated gene expression data using R's glmnet package and performed LASSO-Cox regression analysis [28]. The candidate Imm-DEGs were included in the model, and LASSO algorithm was used for analysis to obtain feature genes associated with IDD. In addition, we also set up a 3-fold cross-validation to obtain the optimal model. The risk scoring formula [Risk Score= (exp-Gene 1 *coef-Gene 1) + … (exp - Gene n *coef - Gene n)] was established using a random forest model to predict the likelihood of IDD. We further evaluated the prognostic value of candidate genes and nomogram through ROC analysis. The area under the curve (AUC) and 95 % confidence interval (CI) were obtained by ROC analysis, where an AUC value > 0.7 was considered to have a good diagnostic effect.

2.7. Immune cell infiltration analysis

The immune microenvironment is usually composed of immune cells, inflammatory cells, fibroblasts, stromal cells, different cytokines, and chemokines. Immune cell infiltration analysis plays an important role in predicting disease progression and treatment response. IOBR [DOI: 10.3389/fimmu.2021.687975] is a immune tumor biology computing tools, Here, based on our expression profile, we used the R software package IOBR and selected xCell (https://doi.org/10.1186/s13059-017-1349-1) method to calculate 64 immunoinfiltrating cell scores for each sample [29]. We used this platform to evaluate the proportions of immune cells between the IDD group and the control group [30]. Heatmaps from the Sangerbox platform were utilized to describe the associations among different immune cells [17].

2.8. In vitro validation experiment

Human nucleus pulposus cells and human myeloid leukemia mononuclear cells (THP-1) were purchased from Procell Life Science&Technology Co., Ltd. (CP–H097, CL-0233). The cells were maintained in Dulbecco's Modified Eagle Medium (11320033 Gibco) containing 10 % fetal bovine serum (29121005 Corning), with an additional 100 U/ml penicillin and 100 mg/ml streptomycin at 37 °C under 5 % CO_2. Firstly, THP-1 were induced by phorbol myristate acetate (100 ng/mL) to differentiate into M0 macrophages. Then the THP-1 macrophages were further induced with LPS (1 μg/mL) for 24 h to differentiate into M1 macrophages. The pre-seeded nucleus pulposus cells were co-cultured with macrophages in the Transwell chamber. The cell supernatant was collected and the expression levels of interleukin-1β (IL- 1β) and tumor necrosis factor-α (TNF-α) in the supernatant of nucleus pulposus cells were detected using IL-1β ELISA kit and TNF-α ELISA kit (LA167616H, LA160102H Nanjing Jin Yibai Biological Technology Co. Ltd.).

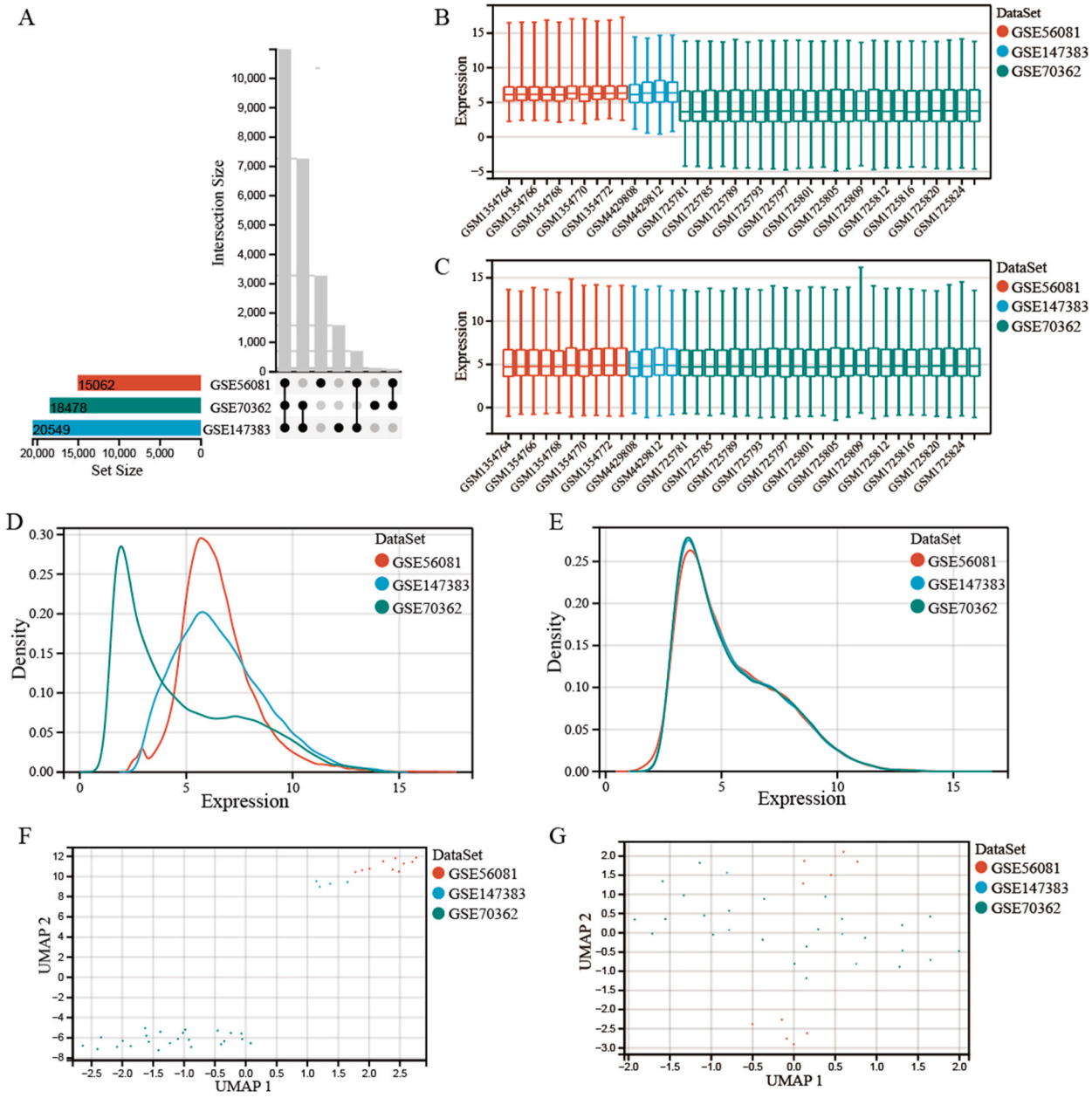

Fig. 1. GEO datasets debatching. (A) Summary of intersections among GEO datasets. (B) Comparison of data set expression distribution before debatching. (C) Comparison of dataset expression distribution after debatching. (D) Comparison of data set density distributions before debatching. (E) Comparison of dataset density distribution after debatching. (F) Unified manifold approximation and projection (UMAP) of data sets before debatching. (G) UMAP of datasets after debatching.

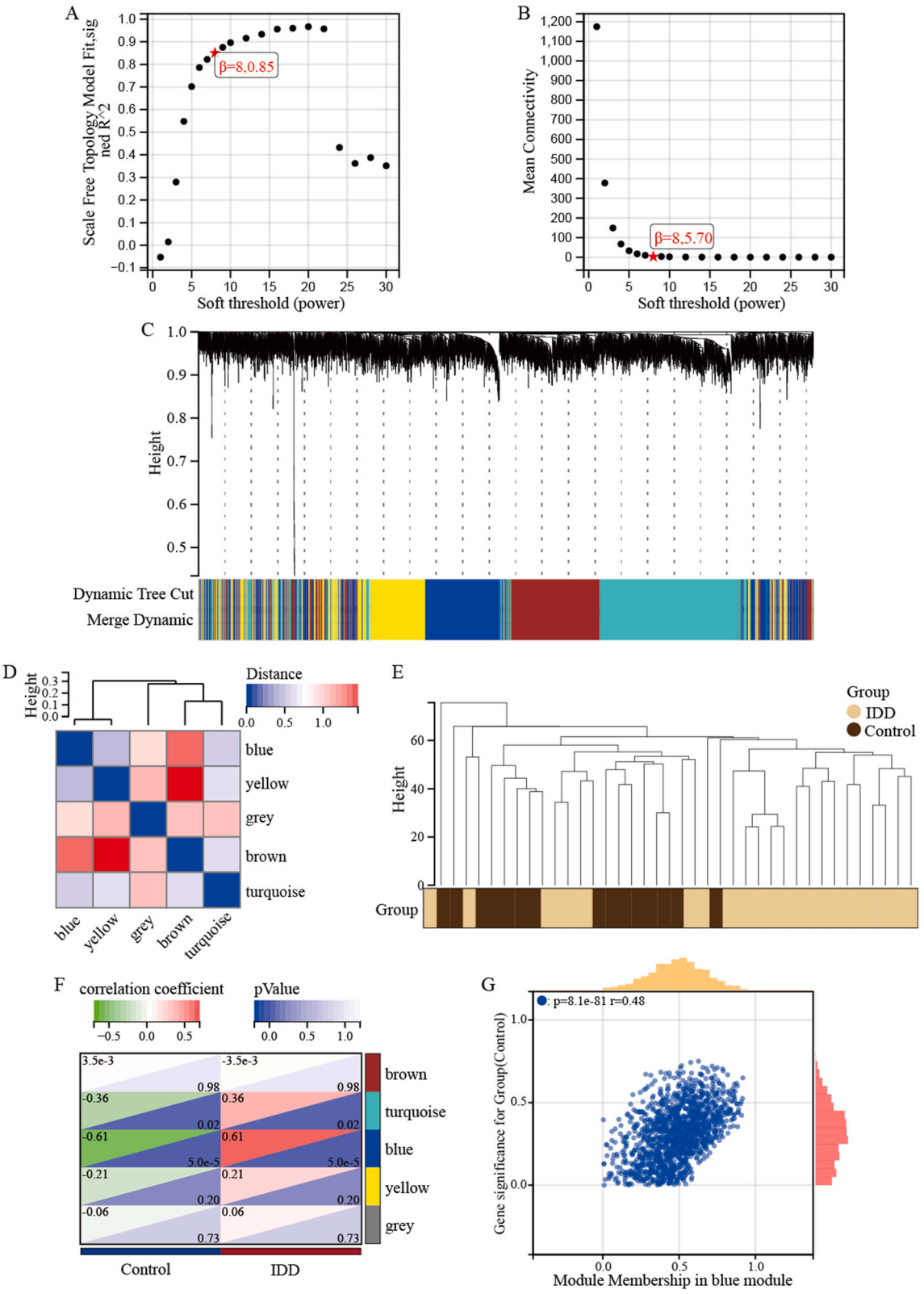

(caption on next page)

Fig. 2. WGCNA and Key Module Identification. (A) The scale-free fit index (scale independence, y-axis) as a function of the soft threshold power (x-axis). (B) The mean connectivity (degree, y-axis) as a function of the soft threshold power (x-axis). (C) Gene dendrograms were obtained by average linkage hierarchical clustering. The colored row underneath the dendrogram shows the module assignment determined by the dynamic tree cut method. (D) Clustering dendrogram of the IDD and control samples. (E) Heatmap of eigengene adjacency. (F) Heatmap of the association between modules and MS. Each cell contains the corresponding correlation and p-value. (G) Correlation plot between module membership and significance of genes included in the blue module.

2.9. Immunofluorescence

M1 macrophages were identified by immunofluorescence. Cells were fixed with 4 % paraformaldehyde, permeabilized with 1 % Triton X-100, and blocked with 3 % goat serum. The CD68 antibody (ARG10514, arigo, 1:200) and iNOS antibody (ARG56509, arigo, 1:200) were added and incubated overnight at 4 °C. The next day, the second antibody was replaced and incubated for 30 min. After incubation, DAPI was used for counterstaining, and fluorescence microscopy was used to visualize the cells.

2.10. Reverse transcription-quantitative real-time PCR (RT-qPCR)

Total RNA was extracted with Trizol. The Optical Density value of the RNA was determined with a spectrophotometer, the purity of the RNA was evaluated, and quantitative analysis was performed. Prime Script RT reagent Kit (Nanjing Nuoweizan Biotechnology Co., LTD., Nanjing China) reverse-transcribed and stored at −20 °C. The corresponding gene sequences in GenBank were retrieved, and the primer was designed using Oligo v6.6 software (Shanghai Bioengineering Technical Service Co., LTD.). The cDNA was amplified with the following primers: GAPDH forward, 5′-GGA GTC CAC TGG CGT CTT CAC-3′; GAPDH reverse, 5′-GCT GAT GAT CTT GAG GCT GTT GTC-3′; NR1H3 forward, 5′-GCC TGA CAT TCC TCC TGA CTC TG-3′; NR1H3 reverse, 5′-GGC ATC CTG GCT TCC TCT CTG- 3′; SORT1 forward, 5′-CTC AGA GCC GAA TGC CGT AGG-3′; SORT1 reverse, 5′-GCC ACA ATG ATG CCT CCA GAA TC-3′; PTGDS forward, 5′-AGA AGA AGG CGG CGT TGT CC-3′; PTGDS reverse, 5′-CAT GGT TCG GGT CTC ACA CTG G-3′; AGT forward, 5′-ACC CTG GCT TTC AAC ACC TAC G-3′; AGT reverse, 5′-TTG AGT CAC CGA GAA GTT GTC CTG-3′; IRF1 forward, 5′-CTC CAC TCT GCC TGA TGA CCA C-3′; IRF1 reverse, 5′-GCC ACT CCG ACT GCT CCA AG-3′; TGFB2 forward, 5′-AGT TCA GAC ACT CAG CAC AGC AG-3′; TGFB2 reverse, 5′-ACG CAG CAA GGA GAA GCA GAT G-3′. 5 × Prime Script RT Master Mix (Nanjing Nuoweizan Biotechnology Co., LTD., Nanjing China) 20ul system was amplified, and the results were calculated as $2^{-\triangle\triangle CT}$ semi-quantitative.

2.11. Western blot

At first, the samples were subjected to protein extraction, and the concentration of protein was assessed utilizing the BCA technique. The proteins were then denatured by heating in a constant-temperature metal bath. Afterwards, additional samples were included according to the protein concentration, subjected to electrophoresis, and then transferred onto a PVDF membrane. At room temperature, the membrane was sealed using 5 % skim milk powder. The following antibodies were added and incubated at 4 °C overnight: NR1H3 antibody (14351-1-AP, proteintech, 1:2000), SORT1 antibody (12369-1-AP, proteintech, 1:2000), PTGDS antibody (10754-2-AP, proteintech, 1:1000), AGT antibody (11992-1-AP, proteintech, 1:1000), IRF1 antibody (11335-1-AP, proteintech, 1:500), TGFB2 antibody (28426-1-AP, proteintech, 1:500), and GAPDH antibody (10494-1-AP, proteintech, 1:5000). On the subsequent day, the second antibody was administered and left to incubate for a duration of 60 min. Finally, ECL chromogenic solution was used for exposure.

2.12. Statistical analysis

Bioinformatics analysis was performed in Sangerbox 3.0 (http://vip.sangerbox.com/home.html) and R software. The chi-square test or Fisher's exact test was carried out to analyze the statistical significance between two sets of categorical variables. Correlation coefficients between different immune cell were estimated via Pearson correlation analysis. The in vitro validation data were analyzed using GraphPad Prism 9.0.0 statistical software. To compare multiple groups, one-way analysis of variance was used. Pairwise comparisons were made using Tukey's test. $P < 0.05$ was considered statistically significant.

3. Results

3.1. Data set processing

Three GEO datasets were de-batch-effect processed to obtain the combined dataset, which included a total of 23 IDD samples and 15 control samples (Fig. 1A). Before de-batch-effect, the sample distribution of each data set in the boxplot and density map is quite different (Fig. 1B and D), and the Unified manifold approximation and projection (UMAP) shows that the samples of each dataset are clustered together (Fig. 1F), indicating that there is a batch effect. After the removal of batch effect, the boxplot shows that the data distribution among all datasets tends to be consistent, and the median is in a line (Fig. 1C); the density map shows that the mean and variance among all datasets are similar (Fig. 1E); and the UMAP shows that the samples among all datasets are clustered and interweaved together (Fig. 1G). The above results indicate that the batch effect is well removed in this study.

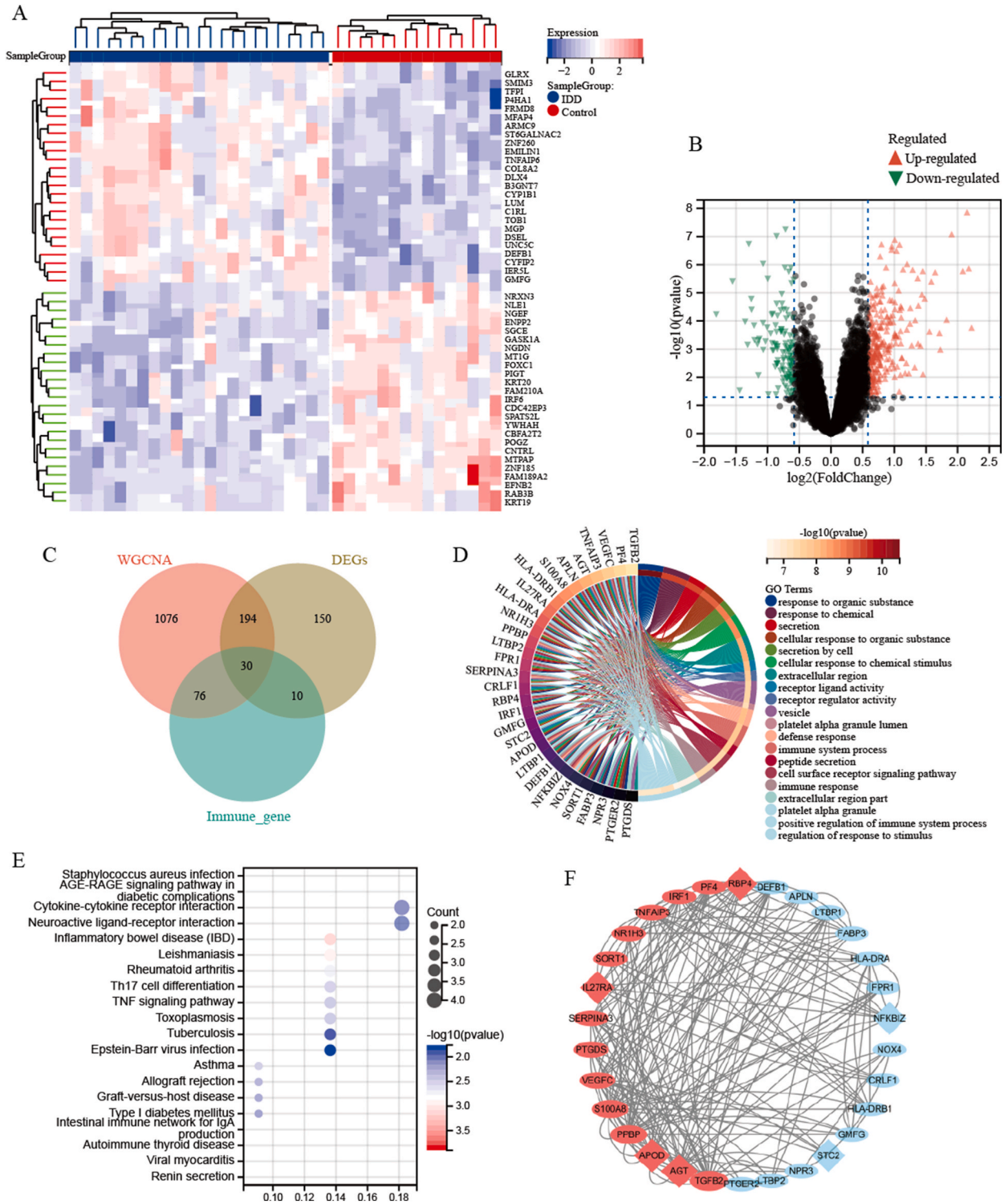

Fig. 3. Expression of immune-related genes in patients with IDD. (A) DEGs expression heatmap (fold change>1.5, *P*-value<0.05). (B) DEGs volcano plot (fold change>1.5, *P*-value<0.05). (C) Genes intersection Venn diagram. (D) GO analysis of the intersection genes. (E) KEGG pathway analysis of the intersection genes. (F) PPI network of Imm-DEGs (ovals represent up-regulated genes, prisms represent down-regulated genes, and red represents core node genes).

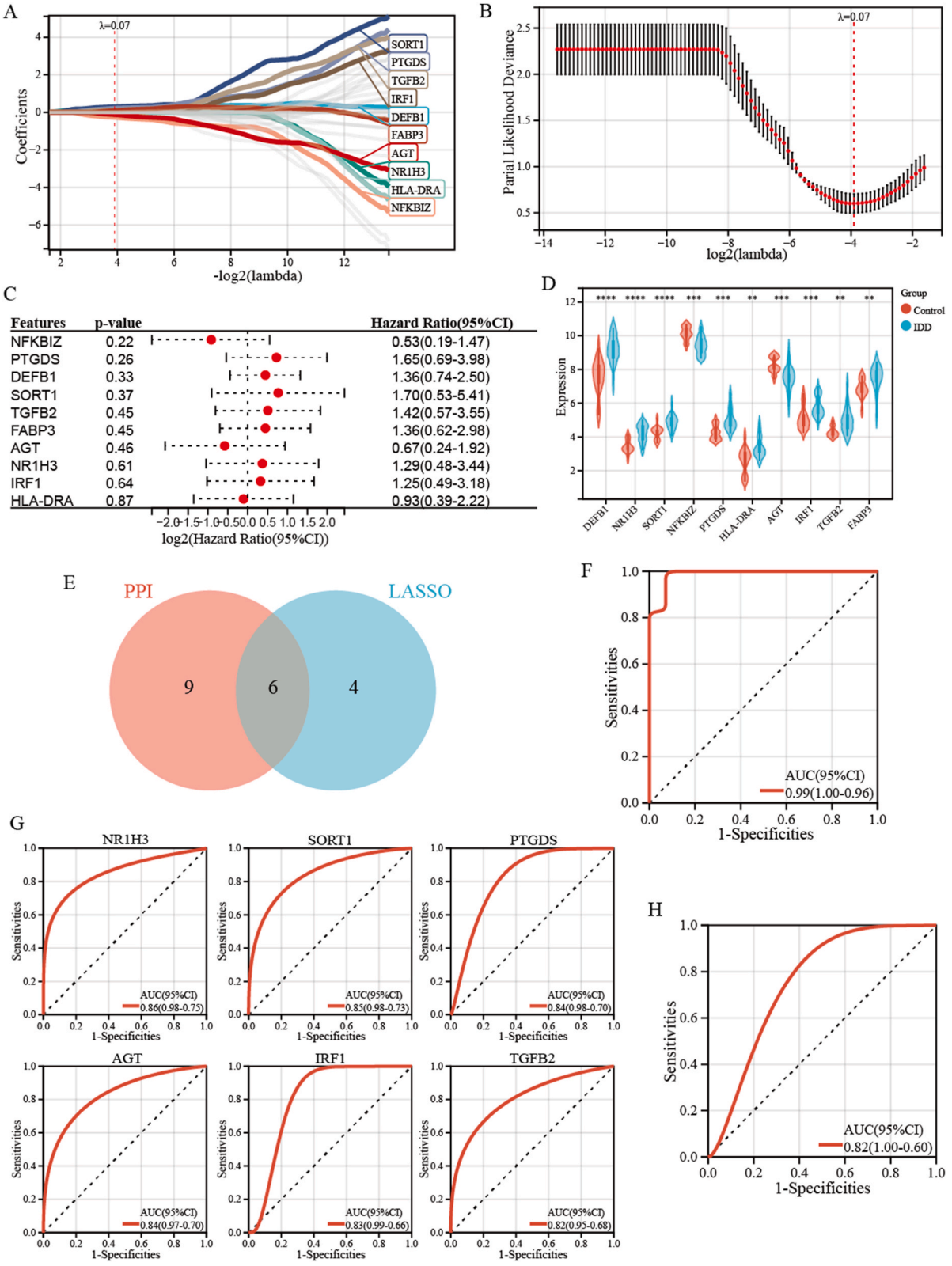

(caption on next page)

Fig. 4. Candidate hub gene identification and diagnosis model construction. (A) Coefficient profiles of variables in the LASSO regression model (Candidate genes: SORT1, PTGDS, TGFB2, IRF1, DEFB1, FABP3, AGT, NR1H3, HLA-DRA, and NFKBIZ). (B) Ten-fold cross-validation for turning parameter (λ) selection in the LASSO regression model. (C) The random forest algorithm of key genes. (D) Violin map of key genes. (E) Venn diagram of the intersection of the LASSO algorithm and core genes in the PPI network. (F) The ROC curve of the diagnostic model. (G) The ROC curve of the individual genes. (H) The ROC curve of the validation dataset.

3.2. WGCNA and Key Module Identification

We used WGCNA to construct a scale-free co-expression network to identify the most relevant module associated with IDD. A "soft" threshold β of 8 was chosen based on scale independence and average connectivity (Fig. 2A and B). Clustering dendrograms were generated for the IDD group and control group, resulting in five different colored gene co-expression modules, as shown in Fig. 2C and D. Correlation analysis results showed that the blue module had the highest correlation with IDD ($r = 0.61$, $P < 0.001$) (Fig. 2E and F). Gene significance and module membership were correlated positively (correlation coefficient = 0.48, $P < 0.001$) in the blue module, consisting of 1375 genes (Fig. 2G). These results indicate that the genes within the blue module are most closely related to IDD.

3.3. Expression of immune-related genes in patients with IDD

Limma gene differential analysis results showed that there were 384 differentially expressed genes between the IDD group and the control group, of which 262 were up-regulated and 122 were down-regulated in the IDD group (Fig. 3A and B). Fig. 3C shows the intersection genes most closely associated with disc degeneration, differential genes, and immune-related genes in a weighted gene co-expression network analysis. Thirty immune-related differentially expressed genes were generated after the IDD group, of which 24 were up-regulated and six were down-regulated. GO analysis elucidated that Imm-DEGs were mainly enriched in biological processes (BP) such as cell reaction, defense response, cell secretion, and immune response, cellular components (CC) such as extracellular matrix and vesicles, and molecular functions (MF) such as receptor ligand activity (Fig. 3D). KEGG analysis showed that Imm-DEGs were primarily enriched in staphylococcus aureus infection, inflammatory bowel disease, rheumatoid arthritis, TGF-beta signaling pathway, IL-17 signaling pathway, and TNF signaling pathway (Fig. 3E). The PPI network of Imm-DEGs consists of 30 nodes and 178

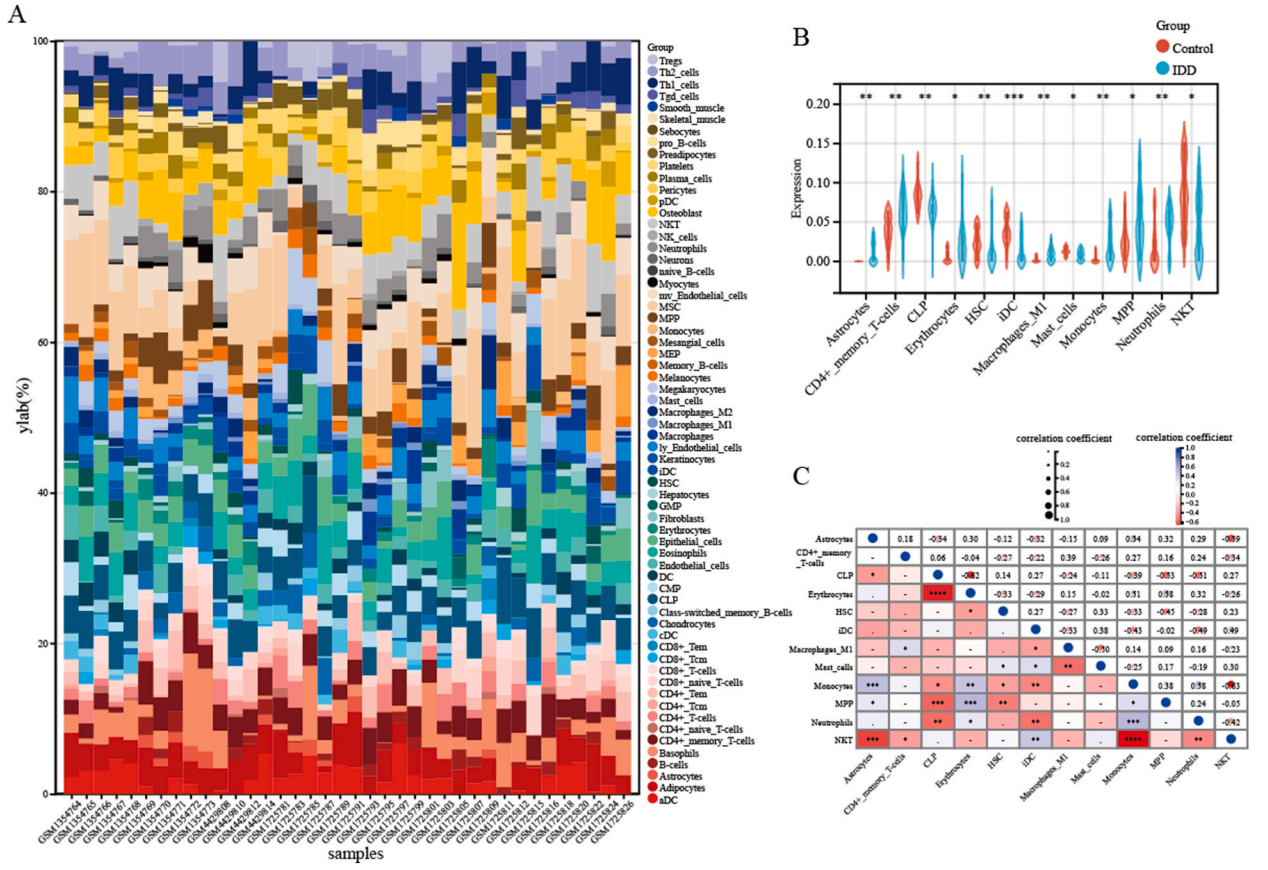

Fig. 5. Immune infiltration analysis. (A) Immune cell content stacking plot. (B) Violin diagram of 12 different immune cells. (C) Correlation matrix of 12 different immune cells.

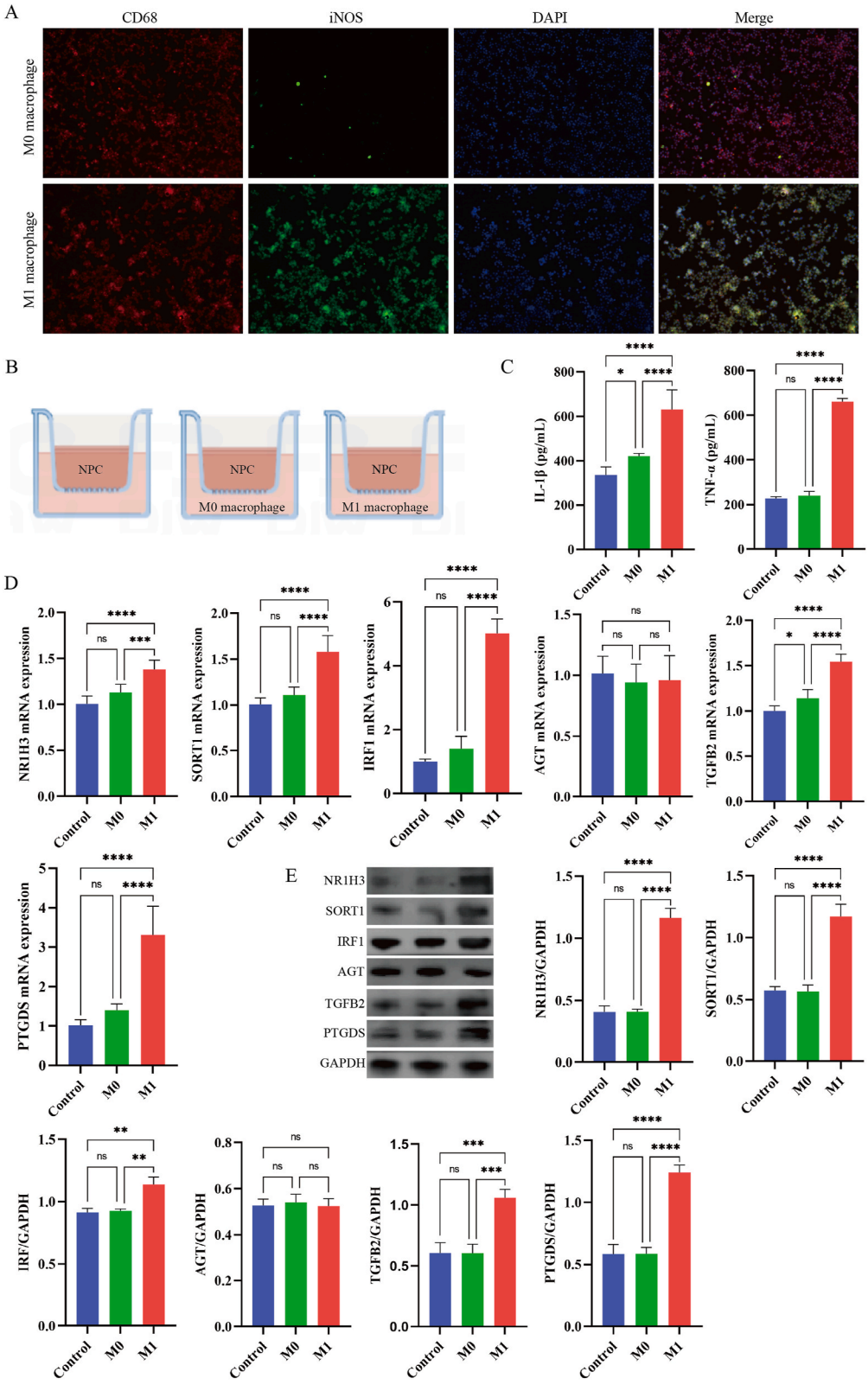

(caption on next page)

Fig. 6. In vitro validation experiment. (A) Identification of M1 macrophages. (B) Cell coculture of nucleus pulposus cells and macrophages. (C) IL-1β and TNF-α levels in the supernatant after 24 h of coculture. (D) Levels of NR1H3, SORT1, PTGDS, AGT, IRF1, and TGFB2 mRNA in nucleus pulposus cells after 24 h of coculture. (E) Levels of NR1H3, SORT1, PTGDS, AGT, IRF1, and TGFB2 protein in nucleus pulposus cells after 24 h of coculture. The unedited images are referenced in Fig. S1. *: $P < 0.05$, **: $P < 0.01$, ***: $P < 0.010$, ****: $P < 0.0001$, ns: $P > 0.05$.

edges (Fig. 3F). Topological analysis shows that core node genes of the network are TGFB2, AGT, APOD, PPBP, S100A8, VEGFC, PTGDS, SERPINA3, IL27RA, SORT1, NR1H3, TNFAIP3, IRF1, PF4, RBP4. By identifying these differentially expressed Imm-DEGs and analyzing their biological functions and enrichment pathways, we can further understand the immunopathological mechanism of IDD, and provide important clues for the prevention, diagnosis and treatment of it.

3.4. Candidate hub gene identification and diagnosis model construction

The LASSO algorithm identified 10 significant feature genes out of 30 Imm-DEGs that have a great impact on IDD (Fig. 4A, B, and C). The expression of these 10 genes in degenerated intervertebral disc samples and control samples is shown in Fig. 4D. The Venn diagram shows the intersection between the candidate genes identified by the LASSO algorithm and the core genes in the PPI network of Imm-DEGs, confirming six genes (NR1H3, SORT1, PTGDS, AGT, IRF1, TGFB2) as HUB genes (Fig. 4E). Based on the coefficients of these six feature genes, the score for IDD was calculated by multiplying the gene expression with the corresponding coefficients and adding them up. Therefore, the formula for the model constructed by the six genes is: RiskScore = 0.149*NR1H3+ 0.296*SORT1+0.210*PTGDS-0.121*AGT+0.085*IRF1+0.124*TGFB2, with a lambda value of 0.06. The receiver operating characteristic (ROC) curves were used to predict IDD based on the six gene features, which showed that all genes had a predictive efficacy of AUC 0.99, 95%CI 0.96–1.00 (Fig. 4F), while individual genes' predictive efficacy was NR1H3 (AUC 0.86, 95%CI 0.75–0.98), SORT1 (AUC 0.85, 95%CI 0.73–0.98), PTGDS (AUC 0.84, 95%CI 0.70–0.98), AGT (AUC 0.84, 95%CI 0.70–0.97), IRF1 (AUC 0.83, 95%CI 0.66–0.99), and TGFB2 (AUC 0.82, 95%CI 0.68–0.95) (Fig. 4G). The predictive effect of all genes was higher than that of individual genes, consistent with the multimolecular driven nature of disc degeneration. The model was validated using GSE124272, which showed a predictive efficacy of AUC 0.82, 95%CI 0.60–1.00 (Fig. 4H), indicating that the model has high diagnostic value for IDD.

3.5. Immune infiltration analysis

Immune infiltration analysis can better explore the role of immunity in IDD, as shown in Fig. 5A for 64 kinds of immune cells in IDD and control groups. The box plot shows that astrocytes, $CD4^+$ memory-activated T cells, erythrocytes, M1 macrophages, monocytes, multipotent progenitors (MPP), and neutrophils levels were higher in the IDD group compared to the control group, while lymphoid progenitor cells (CLP), hematopoietic stem cell (HSC), interdigitating DC (iDC), mast cells, and natural killer T cell (NKT) levels were lower, as shown in Fig. 5B. Analysis of 12 different immune cells showed that astrocytes had a strong correlation with monocytes ($r = 0.54$) and NKT ($r = -0.59$); CLP had a strong correlation with erythrocytes ($r = -0.62$), MPP ($r = -0.53$), and neutrophils ($r = -0.51$); erythrocytes had a strong correlation with monocytes ($r = 0.51$) and MPP ($r = 0.58$); M1 macrophages had a strong correlation with mast cells ($r = -0.50$); monocytes had a strong correlation with neutrophils ($r = 0.58$) and NKT ($r = -0.63$). All correlations are shown in Fig. 5C. In conclusion, different levels of immune cell infiltration in IDD patients may be a potential therapeutic target.

3.6. In vitro validation results

The research suggests that M1 macrophages infiltrate the entire intervertebral disc and trigger a cascade of inflammatory reactions after the destruction of the nucleus pulposus immune barrier, leading to abnormal metabolism of nucleus pulposus cells and degradation of extracellular matrix [31,32]. They are one of the important immune cells involved in IDD. Immune infiltration analysis also shows an increase in M1 macrophage levels in the nucleus pulposus tissue of degenerative discs. Therefore, we co-cultured nucleus pulposus cells with macrophages to create an M1-polarized immune inflammatory environment and verify changes in HUB genes. iNOS is one of the commonly used markers for M1 macrophages, and immunofluorescence results show that LPS can successfully induce M1 macrophage polarization. (Fig. 6A). After co-culturing nucleus pulposus cells with M1 macrophages for 24 h, the levels of IL-1β and TNF-α in the cell supernatant were significantly increased, indicating that the nucleus pulposus cells were in an immune inflammatory environment. (Fig. 6B and C). The expression of NR1H3, SORT1, PTGDS, IRF1, and TGFB2 in nucleus pulposus cells was upregulated when they were exposed to the immune inflammatory environment, which is consistent with previous bioinformatics analysis results. However, downregulation of AGT was not significant, indicating that the expression of AGT in nucleus pulposus cells may be regulated by other factors. (Fig. 6D, E and Fig. S1).

4. Discussion

Intervertebral discs are the largest avascular enclosed structures in the human body and have been isolated from autologous blood circulation since birth, making them inherently antigenic. The annulus fibrosus and the cartilaginous endplate constitute a solid physical barrier that separates the nucleus pulposus tissue in the intervertebral disc from the body's immune system, preventing immune cells and immune factors from entering the intervertebral disc. Fas ligands were found in the nucleus pulposus of the intervertebral disc. Fas ligands, as apoptosis-inducing factors, are widely expressed in other immune pardoning organs. Fas ligands

may function as molecular barriers by inhibiting vascular and immune cell infiltration [7,33]. In addition, many studies have reported the protective role of notochordal cells in intervertebral disc and their inhibitory effect on inflammation [34]. In summary, the annulus fibrosus, the cartilage endplate, and certain biological factors, such as Fas ligands, together constitute a unique structure that maintains intervertebral disc immunity [35]. When the annulus fibrosus ruptures and the isolation function disappears, the body recognizes the nucleus pulposus as "non-self" tissue, and the isolated antigens in the nucleus pulposus come into contact with the body's immune system, resulting in an autoimmune reaction that is the main cause of the inflammatory reaction in intradiscal tissue [5,6]. Understanding the pathogenesis of IDD at the level of immune molecules will provide a theoretical basis for us to comprehensively and deeply understand the pathological process of this disease and develop more effective prevention and treatment measures. Therefore, we used bioinformatics analysis and machine learning methods to identify immunorelated diagnostic candidate genes for IDD. We identified six key immunorelated candidate genes (NR1H3, SORT1, PTGDS, AGT, IRF1, TGFB2) and performed in vitro experiments to validate them. Experimental results showed that the gene expression of NR1H3, SORT1, PTGDS, IRF1, and TGFB2 in nucleus pulposus cells in the immune inflammatory environment was up-regulated, consistent with bioinformatics analysis results, but the change of AGT was not significant.

The protein encoded by the nuclear receptor subfamily 1 group H member 3 (NR1H3) gene belongs to the NR1 subfamily of the nuclear receptor superfamily, also known as the liver X receptor-α (LXRα). NR1 family members are key regulatory factors for macrophage function, involved in controlling lipid homeostasis and transcriptional programs relating to inflammation. When LXRα is activated by inflammatory substances, it quickly enters the nucleus from the cytoplasm and is modified by small ubiquitin-like modifier proteins [36]. At the same time, LXRα recruits nuclear receptor co-repressor (N-CoR) in the nucleus, initiating a "transcriptional repression" mechanism that affects the expression of inflammatory genes and the stimulation of chemokines by regulating signaling pathways such as nuclear factor-κB (NF-κB), toll-like receptors, etc [37]. For example, Jeon et al. showed that the polymorphism of the LXRα promoter region (1830 T > C) is associated with an increased risk of systemic lupus erythematosus and corresponded to decreased expression of LXRα in B cells [38]. Other studies demonstrated that LXR expression was elevated in $CD4^+$ T cells of patients with SLE [39] and macrophages in synovial fluid of rheumatoid arthritis patients [40], which are believed to be the cause of aberrant immune responses. In summary, these studies support the role of LXR in the immune system and suggest that abnormal LXR signaling (increased or decreased) may lead to immune cell dysfunction, especially autoimmune disorders.

Sortilin1 (SORT1) participates in innate immunity by regulating inflammation and phagocytosis, and in adaptive immunity by controlling immune cell maturation and regulating T cell and NK cell activation [41]. At present, there has been little research on the role of SORT1 in immune regulation; further understanding of this gene may reveal new functions in immune regulatory pathways.

Prostaglandin D2 synthase (PTGDS), also known as PGD2 or L-PGDS, is a major prostaglandin and an important mediator of allergic responses. PGD2 is the primary product of COX catalytic reactions in various tissues and cells, including T cells, DCs, macrophages, mast cells, and platelets [42]. PGD2 also acts as a neuromodulator and trophic factor in the central nervous system [43]. Studies have shown that after the injury of sciatic nerve and dorsal root ganglion neurons, PGD2 regulates the phagocytosis activity of macrophages through non-cellular autonomous mechanisms, promotes the removal of myelin debris and conducive to axon and myelin regeneration. In addition, PGD2 regulates blood pressure barrier permeability and SOx2 expression levels in Schwann cells, controlling macrophage accumulation in injured nerves [44]. Therefore, we speculate that PGD2 may also influence IDD by regulating the focusing and function of immune cells such as macrophages.

The activation of interferon regulatory factor 1 (IRF1) is involved in the transcription of genes that respond to viruses and bacteria in humans and it plays a role in cellular proliferation, apoptosis, immune response, and DNA damage response. The IRF1 gene is generally expressed at low basal levels in cells and is highly sensitive to various stimuli, including interferons and NF-κB [45]. The high expression of IRF1 in degenerated intervertebral discs also provides evidence for the theory of autoimmune-mediated IDD.

Transforming growth factor-beta 2 (TGFB2) is a member of the TGF-β superfamily of proteins that regulate cell growth and differentiation. TGF-β is a pleiotropic cytokine that has both positive and negative effects on various tissues and disease states, suggesting that overactivation of TGF-β signaling may further lead to IVD degradation [46,47]. The TGF-β cytokine family contains multiple subtypes, including TGFB1, TGFB2, and TGFB3, which have similar effects on various cells, such as macrophages, T cells, and B cells [48]. In the early stages of inflammation, preexisting latent TGFB2 and TGFB2 released from the site of injury bind to local extracellular matrix and become activated. The activated TGFB2 has strong chemotactic properties for leukocytes, monocytes, T cells, and fibroblasts [49]. Currently, TGFB2 is considered an immune-regulatory factor that is closely related to maintaining the immunosuppressive environment and immune privilege in the eye [50]. The nucleus pulposus also has immunoprivileged characteristics; thus, there is reason to believe that TGF-β2 may also play an important role as an immune-regulatory factor in the process of IDD.

As the main functional executors of the immune system, immune cells participate widely in the occurrence and progression of degenerative diseases. Degenerated nucleus pulposus cells and annulus fibrosus cells produce a large amount of proinflammatory cytokines, including IL-1α, IL-1β, TNF-α and C–C motif chemokine ligand (CCL), etc [51]. These inflammatory chemotactic factors further recruit immune cells to infiltrate the intervertebral disc and aggravate the inflammatory response. Our research shows that astrocytes, $CD4^+$ memory-activated T cells, M1 macrophages, monocytes, neutrophils, etc., are present at higher levels in degenerated discs [52]. Macrophages are the main type of inflammatory cells in degenerated intervertebral disc tissue. Macrophages are important defense functional immune cells differentiated from monocytes in the blood, mainly playing a role in phagocytosis, antigen presentation, and secretion of cytokines during immune responses. M1 macrophages have the function of antigen presentation and secretion of proinflammatory cytokines. Normal intervertebral disc tissues are excluded from the immune system, and T cells cannot be detected. When IDD occurs, the disc nucleus itself can activate T cell subsets, leading to an imbalance of T cell subsets and an outbreak of inflammation [53]. According to the differentiation antigens on the cell surface, mature T lymphocyte cells can be divided into two subtypes: $CD4^+$ and $CD8^+$. $CD4^+$ T cells recognize exogenous antigen peptides composed of 13–17 amino acids and mainly

differentiate into helper T cells (Th) after activation, which can help B cells produce antibodies, form antigen-antibody complexes, and exacerbate the inflammatory response [54]. At first, it was thought that macrophages might be the only immune cells infiltrating the intervertebral disc [55]. Later studies have shown that there are different types of immune cell infiltration in the degenerative disc, but most studies have focused on the relationship between macrophages and disc degeneration. Our study showed that in addition to M1 macrophages, immune cells such as T cells and neutrophils also play an important role in the immune inflammatory response of intervertebral disc, suggesting the direction of future research. At present, many immunotherapy drugs used in tumor play an immunotherapeutic role by regulating immune infiltrating cells such as macrophages and T cells [56]. These results indicate that there is a close relationship between IDD and immune system changes, and regulating immune-infiltrating cells may become a therapeutic target for IDD [57].

Molecular markers can indicate biological changes, and the changes in the biomarker spectrum detected in degenerated intervertebral discs and peripheral blood may play an important role in early detection of IDD [58]. Diagnostic value analysis indicates that the diagnostic model we constructed has high accuracy and stability in diagnosing intervertebral disc degeneration in both the training queue and peripheral blood verification queue. However, clinical validation is needed to identify these genes as potential therapeutic targets or diagnostic markers. This includes evaluating the efficacy of drugs targeting the central gene in clinical trials or validating the accuracy and clinical application value of diagnostic markers. After clinical verification, on the one hand, the expression pattern of the central gene can be used to develop relevant diagnostic markers or biomarkers for diagnosis, prediction of disease course or evaluation of treatment effect. On the one hand, based on specific expression patterns of central genes, drugs can be developed to target these genes to regulate the immune response and the process of IDD.

Due to the limited datasets meeting the criteria, the included datasets and samples could not cover groups with different races, genders, ages and degrees of degeneration. Therefore, the influence of these factors on gene expression was not explored in this study, which has an impact on the robustness of the study results. More original studies and bioinformatics studies involving different races, ages and genders are needed in the future.

5. Conclusion

In this study, we successfully identified five immune-related hub genes (NR1H3, SORT1, PTGDS, IRF1, TGFB2) using bioinformatics analysis, machine learning algorithms, and experimental verification. These hub genes have significant specificity and have shown important roles in immune-related functional annotation and pathway analysis, revealing the immunoinflammatory regulation mechanism of disc degeneration. These genes have shown potential as diagnostic candidate genes for IDD and are potential targets for immunoregulatory therapy. Overall, our research results may provide new insights into the pathogenesis of IDD.

Funding

This work was supported by the National Natural Science Foundation of China (82174399), Jiangsu Provincial Department of Science and Technology (BK20211084), Jiangsu Provincial Bureau of Traditional Chinese Medicine Program (QN202007); Suzhou Science and Technology Bureau Project (SYS2020183; SKYXD2022042), Construction project of Key Laboratory of Bone Injury Science of Traditional Chinese Medicine (JSDW202253, SZS2022019).

Data availability statement

The datasets analyzed during the current study are available in the GEO repository: https://www.ncbi.nlm.nih.gov/geo/query/acc.cgi?acc=GSE70362
https://www.ncbi.nlm.nih.gov/geo/query/acc.cgi?acc=GSE147383
https://www.ncbi.nlm.nih.gov/geo/query/acc.cgi?acc=GSE56081
https://www.ncbi.nlm.nih.gov/geo/query/acc.cgi?acc=GSE124272.

Ethics approval and consent to participate

This study does not involve ethical approval.

Consent for publication

Not applicable.

CRediT authorship contribution statement

Zeling Huang: Writing – original draft, Visualization, Project administration, Formal analysis, Data curation, Conceptualization. **Xuefeng Cai:** Writing – original draft, Methodology, Formal analysis, Conceptualization. **Xiaofeng Shen:** Writing – original draft, Methodology, Conceptualization. **Zixuan Chen:** Visualization, Formal analysis. **Qingtian Zhang:** Software, Investigation. **Yujiang Liu:** Validation, Investigation. **Binjie Lu:** Validation, Investigation. **Bo Xu:** Writing – review & editing, Supervision, Resources, Project administration, Conceptualization. **Yuwei Li:** Writing – review & editing, Supervision, Resources, Project administration,

Conceptualization.

Declaration of competing interest

The authors declare that they have no known competing financial interests or personal relationships that could have appeared to influence the work reported in this paper.

Acknowledgments

We thank for the help provided by the Key Laboratory for Metabolic Diseases in Chinese Medicine, First College of Clinical Medicine, Nanjing University of Chinese Medicine, and the language editing service for Home for Researchers editorial team (www.home-for-researchers.com).

List of abbreviations

IDD	Intervertebral disc degeneration
GEO	Gene Expression Omnibus
Limma	Linear models for microarray data analysis
WGCNA	Weighted gene correlation network analysis
ROC	Receiver operating characteristic
PPI	Protein-Protein Interaction
IL- 1β	Interleukin-1β
TNF-α	Tumor necrosis factor-α
NR1H3	Nuclear receptor subfamily 1 group H member 3
SORT1	Sortilin1
PTGDS	Prostaglandin D2 synthase
IRF1	Interferon regulatory factor 1
TGFB2	Transforming growth factor-beta 2

Appendix A. Supplementary data

Supplementary data to this article can be found online at https://doi.org/10.1016/j.heliyon.2024.e34530.

References

[1] N.N. Knezevic, K.D. Candido, J.W.S. Vlaeyen, Z.J. Van, S.P. Cohen, Low back pain, Lancet. 398 (10294) (2021) 78–92.
[2] IsaIL. Mohd, S.L. Teoh, NorNH. Mohd, S.A. Mokhtar, Discogenic low back pain: anatomy, pathophysiology and treatments of intervertebral disc degeneration, Int. J. Mol. Sci. 24 (1) (2022) 208.
[3] S. Kirnaz, C. Capadona, T. Wong, J.L. Goldberg, B. Medary, F. Sommer, et al., Fundamentals of intervertebral disc degeneration, World Neurosurg 157 (2022) 264–273.
[4] T. Ohnishi, N. Iwasaki, H. Sudo, Causes of and molecular targets for the treatment of intervertebral disc degeneration: a review, Cells 11 (3) (2022) 394.
[5] Z. Sun, B. Liu, Z.J. Luo, The immune privilege of the intervertebral disc: implications for intervertebral disc degeneration treatment, Int. J. Med. Sci. 17 (5) (2020) 685–692.
[6] C. Song, W. Cai, F. Liu, K. Cheng, D. Guo, Z. Liu, An in-depth analysis of the immunomodulatory mechanisms of intervertebral disc degeneration, JOR Spine 5 (4) (2022) e1233.
[7] Z.H. Liu, Z. Sun, H.Q. Wang, J. Ge, T.S. Jiang, Y.F. Chen, et al., FasL expression on human nucleus pulposus cells contributes to the immune privilege of intervertebral disc by interacting with immunocytes, Int. J. Med. Sci. 10 (8) (2013) 1053–1060.
[8] J.G. Burke, R.W. Watson, D. McCormack, F.E. Dowling, M.G. Walsh, J.M. Fitzpatrick, Intervertebral discs which cause low back pain secrete high levels of proinflammatory mediators, J Bone Joint Surg Br 84 (2) (2002) 196–201.
[9] R. Li, L. Li, Y. Xu, J. Yang, Machine learning meets omics: applications and perspectives, Briefings Bioinf. 23 (1) (2022) bbab460.
[10] D. Liu, Z. Liu, J. Zhang, Y. Yin, J. Xi, L. Wang, et al., Classification and Prediction of Skyrmion Material Based on Machine Learning, 6, Research (Wash D C), 2023, p. 82.
[11] N. Bupi, V.K. Sangaraju, L.T. Phan, A. Lal, T.T.B. Vo, P.T. Ho, et al., An Effective Integrated Machine Learning Framework for Identifying Severity of Tomato Yellow Leaf Curl Virus and Their Experimental Validation, 6, Research (Wash D C), 2022, p. 16.
[12] Y. Fu, Z. Ling, H. Arabnia, Y. Deng, Current trend and development in bioinformatics research, BMC Bioinf. 21 (2020) 538.
[13] Z. Kazezian, R. Gawri, L. Haglund, J. Ouellet, F. Mwale, F. Tarrant, et al., Gene expression profiling identifies interferon signalling molecules and IGFBP3 in human degenerative annulus fibrosus, Sci. Rep. 5 (2015) 15662, 2015 Oct 22.
[14] V. Tam, P. Chen, A. Yee, N. Solis, T. Klein, M. Kudelko, et al., DIPPER, a spatiotemporal proteomics atlas of human intervertebral discs for exploring ageing and degeneration dynamics, Elife 9 (2020) e64940.
[15] P.H. Lan, Z.H. Liu, Y.J. Pei, Z.G. Wu, Y. Yu, Y.F. Yang, et al., Landscape of RNAs in human lumbar disc degeneration, Oncotarget 7 (39) (2016) 63166–63176.
[16] Y. Wang, G. Dai, L. Li, L. Liu, L. Jiang, S. Li, et al., Transcriptome signatures reveal candidate key genes in the whole blood of patients with lumbar disc prolapse, Exp. Ther. Med. 18 (6) (2019) 4591–4602.
[17] W. Shen, Z. Song, X. Zhong, M. Huang, D. Shen, P. Gao, et al., Sangerbox: a comprehensive, interaction-friendly clinical bioinformatics analysis platform, iMeta 1 (2022) e36.
[18] R. Edgar, M. Domrachev, A.E. Lash, Gene Expression Omnibus: NCBI gene expression and hybridization array data repository, Nucleic Acids Res. 30 (2002) 207–210.

[19] W.E. Johnson, C. Li, A. Rabinovic, Adjusting batch effects in microarray expression data using empirical Bayes methods, Biostatistics 8 (1) (2007) 118–127.
[20] S. Bhattacharya, P. Dunn, C.G. Thomas, B. Smith, H. Schaefer, J. Chen, et al., ImmPort, toward repurposing of open access immunological assay data for translational and clinical research, Sci. Data 5 (2018) 180015.
[21] G. Stelzer, N. Rosen, I. Plaschkes, S. Zimmerman, M. Twik, S. Fishilevich, et al., The GeneCards suite: from gene data mining to disease genome sequence analyses, Curr Protoc Bioinf 54 (1.30) (2016) 31–31.30.33.
[22] P. Langfelder, S. Horvath, WGCNA: an R package for weighted correlation network analysis, BMC Bioinf. 9 (2008) 559.
[23] M.E. Ritchie, B. Phipson, D. Wu, Y. Hu, C.W. Law, W. Shi, et al., Limma powers differential expression analyses for RNA-sequencing and microarray studies, Nucleic Acids Res. 43 (2015) e47.
[24] G. Yu, L.G. Wang, Y. Han, Q.Y. He, Clusterprofiler: an R Package for Comparing Biological Themes Among Gene Clusters, 16, Omics, 2012, pp. 284–287.
[25] M.D. Wilkerson, D.N. Hayes, Consensus cluster plus: a class discovery tool with confidence assessments and item tracking, Bioinformatics 26 (2010) 1572–1573.
[26] M. Kanehisa, S. Goto, KEGG: kyoto encyclopedia of genes and genomes, Nucleic Acids Res. 28 (2000) 27–30.
[27] P. Shannon, A. Markiel, O. Ozier, N.S. Baliga, J.T. Wang, D. RamageGene Expression Omnibus, NCBI gene expression and hybridization array data repository. Cytoscape: a software environment for integrated models of biomolecular interaction networks, Genome Res. 13 (11) (2003) 2498–2504.
[28] C. Yang, C. Delcher, E. Shenkman, S. Ranka, Machine learning approaches for predicting high cost high need patient expenditures in health care, Biomed. Eng. Online 17 (2018) 131.
[29] D. Aran, Z. Hu, A.J. Butte xCell, Digitally portraying the tissue cellular heterogeneity landscape, Genome Biol. 18 (1) (2017) 220.
[30] A.M. Newman, C.L. Liu, M.R. Green, A.J. Gentles, W. Feng, Y. Xu, et al., Robust enumeration of cell subsets from tissue expression profiles, Nat. Methods 12 (2015) 453–457.
[31] P. Feng, Y. Che, C. Gao, L. Zhu, J. Gao, N.V. Vo, Immune exposure: how macrophages interact with the nucleus pulposus, Front. Immunol. 14 (2023) 1155746.
[32] X.C. Li, S.J. Luo, F. Wu, Q.C. Mu, J.H. Yang, C. Jiang, et al., Investigation of macrophage polarization in herniated nucleus pulposus of patients with lumbar intervertebral disc herniation, J. Orthop. Res. 41 (6) (2023) 1335–1347.
[33] Z. Sun, Z.Y. Wan, Y.S. Guo, H.Q. Wang, Z.J. Luo, FasL on human nucleus pulposus cells prevents angiogenesis in the disc by inducing Fas-mediated apoptosis of vascular endothelial cells, Int. J. Clin. Exp. Pathol. 6 (11) (2013) 2376–2385.
[34] F.C. Bach, A.R. Tellegen, M. Beukers, A. Miranda-Bedate, M. Teunissen, W.A.M. de Jong, et al., Biologic canine and human intervertebral disc repair by notochordal cell-derived matrix: from bench towards bedside, Oncotarget 9 (41) (2018) 26507–26526.
[35] Z. Xu, Z.J. Luo, Z. Sun, Intervertebral disc:a neglected immune-privileged organ, Journal of Air Force Medical University 12 (1) (2021) 42–46, https://doi.org/10.13276/j.issn.1674-8913.2021.01.009.
[36] K.E. Waddington, E.C. Jury, I. Pineda-Torra, Liver X receptors in immune cell function in humans, Biochem. Soc. Trans. 43 (4) (2015) 752–757.
[37] N. Li, Y. Li, X. Han, J. Zhang, J. Han, X. Jiang, et al., LXR agonist inhibits inflammation through regulating MyD88 mRNA alternative splicing, Front. Pharmacol. 13 (2022) 973612.
[38] J.Y. Jeon, J.Y. Nam, H.A. Kim, Y.B. Park, S.C. Bae, C.H. Suh, Liver X receptors alpha gene (NR1H3) promoter polymorphisms are associated with systemic lupus erythematosus in Koreans, Arthritis Res. Ther. 16 (3) (2014) R112.
[39] G. McDonald, S. Deepak, L. Miguel, C.J. Hall, D.A. Isenberg, A.I. Magee, et al., Normalizing glycosphingolipids restores function in CD4+ T cells from lupus patients, J. Clin. Invest. 124 (2) (2014) 712–724.
[40] D.L. Asquith, L.E. Ballantine, J.S. Nijjar, M.K. Makdasy, S. Patel, P.B. Wright, et al., The liver X receptor pathway is highly upregulated in rheumatoid arthritis synovial macrophages and potentiates TLR-driven cytokine release, Ann. Rheum. Dis. 72 (12) (2013) 2024–2031.
[41] H. Talbot, S. Saada, T. Naves, P.F. Gallet, A.L. Fauchais, M.O. Jauberteau, Regulatory roles of sortilin and SorLA in immune-related processes, Front. Pharmacol. 9 (2019 Jan 7) 1507.
[42] M. Arima, T. Fukuda, Prostaglandin D_2 and T(H)2 inflammation in the pathogenesis of bronchial asthma, Korean J Intern Med 26 (1) (2011) 8–18.
[43] A.S. Ahmad, H. Ottallah, C.B. Maciel, M. Strickland, S. Doré, Role of the L-PGDS-PGD2-DP1 receptor axis in sleep regulation and neurologic outcomes, Sleep 42 (6) (2019) zsz073.
[44] M.G. Forese, M. Pellegatta, P. Canevazzi, G.S. Gullotta, P. Podini, C. Rivellini, et al., Prostaglandin D2 synthase modulates macrophage activity and accumulation in injured peripheral nerves, Glia 68 (1) (2020) 95–110.
[45] H. Feng, Y.B. Zhang, J.F. Gui, S.M. Lemon, D. Yamane, Interferon regulatory factor 1 (IRF1) and anti-pathogen innate immune responses, PLoS Pathog. 17 (1) (2021) e1009220.
[46] Q. Bian, A. Jain, X. Xu, K. Kebaish, J.L. Crane, Z. Zhang, et al., Excessive activation of TGFβ by spinal instability causes vertebral endplate sclerosis, Sci. Rep. 6 (2016) 27093.
[47] S. Chen, S. Liu, K. Ma, L. Zhao, H. Lin, Z. Shao, TGF-β signaling in intervertebral disc health and disease, Osteoarthritis Cartilage (2019) 1109–1117.
[48] K. Tzavlaki, A. Moustakas, TGF-B signaling, Biomolecules 10 (3) (2020) 487.
[49] E. Batlle, J. Massagué, Transforming growth factor-β signaling in immunity and cancer, Immunity 50 (4) (2019) 924–940.
[50] S.E. Wilson, TGF beta -1, -2 and -3 in the modulation of fibrosis in the cornea and other organs, Exp. Eye Res. 207 (2021) 108594.
[51] G.I. Cosamalón, G.T. Cosamalón, P.G. Mattos, S.V. Villar, C.J. García, Á.J. Vega, Inflammation in the intervertebral disc herniation, Neurocirugia (Astur : Engl Ed). 32 (1) (2021) 21–35.
[52] J. Koroth, E.O. Buko, R. Abbott, C.P. Johnson, B.M. Ogle, L.S. Stone, et al., Macrophages and intervertebral disc degeneration, Int. J. Mol. Sci. 24 (2) (2023) 1367.
[53] L. Cheng, W. Fan, B. Liu, X. Wang, L. Nie, Th17 lymphocyte levels are higher in patients with ruptured than non-ruptured lumbar discs, and are correlated with pain intensity, Injury 44 (12) (2013) 1805–1810.
[54] Y. Feng, X. Yang, Y.K. Wang, The relationship between degenerative diseases of lumbar intervertebral disc and peripheral blood lymphocyte subsets, Tissue engineering Research in China 24 (17) (2020) 2630–2635.
[55] C. Yang, P. Cao, Y. Gao, M. Wu, Y. Lin, Y. Tian, W. Yuan, Differential expression of p38 MAPK α, β, γ, δ isoforms in nucleus pulposus modulates macrophage polarization in intervertebral disc degeneration, Sci. Rep. 6 (2016) 22182.
[56] S. Dong, X. Guo, F. Han, Z. He, Y. Wang, Emerging role of natural products in cancer immunotherapy, Acta Pharm. Sin. B 12 (3) (2022) 1163–1185.
[57] C. Dong, Cytokine regulation and function in T cells, Annu. Rev. Immunol. 39 (2021) 51–76.
[58] A. Kamali, R. Ziadlou, G. Lang, J. Pfannkuche, S. Cui, Z. Li, et al., Small molecule-based treatment approaches for intervertebral disc degeneration: current options and future directions, Theranostics 11 (1) (2021) 27–47.